Powder Alloying and Spheroidization^{SM}

J.S. O'Dell, E.C. Schofield, R. Hickman, T.N. McKechnie, C. Power
Plasma Processes, Inc., Huntsville, Alabama, USA

Abstract

Elemental, blended, and coated refractory metal powders were processed using a powder alloying and spheroidization (PAS^{SM}) process. The powders were characterized to determine changes in chemistry and morphology after processing. Five refractory metal powders were evaluated during this investigation: 1) crystalline tungsten, 2) spray dried molybdenum, 3) W-25%Re composite powder, 4) Mo-40%Re composite powder, and 5) Mo-40%Re coated powder. One non-refractory metal powder, Ti-6%Al-4%V was processed as well. Benefits of PAS^{SM} such as reduced oxygen content, highly spherical powders with enhanced flow, and production of pre-alloyed powders were demonstrated.

Introduction

Free-flowing powder feedstock is desired to improve process repeatability and handling for many applications. In addition, pre-alloyed powders are desired.[1-3] To address these issues, Powder Alloying and Spheroidization (PAS^{SM}) has been developed and evaluated to produce spherical and pre-alloyed powders.[4-5]

During Powder Alloying and Spheroidization (PAS^{SM}), powder feedstock is fed into a plasma where melting occurs and surface tension causes spherical droplets to form. During this molten stage, alloying takes place. As the droplets pass out of the plasma, they rapidly solidify and are collected. To minimize oxidation of feedstock during processing, PAS^{SM} is conducted in vacuum or inert atmosphere for oxygen sensitive materials. For less oxygen sensitive materials, PAS^{SM} is performed at ambient conditions. Auxiliary cooling gases are incorporated to enhance powder cooling if necessary.

Typically, an inert gas such as argon is used to form the plasma. Secondary gases, such as hydrogen, are used to promote higher temperature plasmas and reduce oxide scale on the surface of powder feedstock.

Experimental Procedure

Five refractory metal powders and one non-refractory metal powder were evaluated during this investigation: 1) crystalline tungsten, 2) spray dried molybdenum, 3) W-25%Re composite powder, 4) Mo-40%Re composite powder, 5) Mo-40%Re coated composite powder, and 6) Ti-6%Al-4%V. Because refractory metals and Ti alloys are sensitive to oxidation, these powders were PAS^{SM} processed in vacuum and inert atmospheres. Detailed descriptions of the powders are given in Table 1.

Table 1: Description of starting powders.

Composition	Description	Particle Size (μm)
W	Crystalline	-45
W-25Re	Composite*	-45/+15
Mo	Spray dried	-38
Mo-40Re	Composite*	-45/+15
Mo-40Re	Re-Coated, Spray dried Mo	-45/+15
Ti-6Al-4V	Pre-alloyed, crushed	-45/+15

* - Elemental blend with 1-2% organic binder.

The Hall flow test was used to characterize the flowability of refractory metal powders. This test measures the time required for a specific amount of powder to pass through a critical orifice as a result of gravity.

Both optical and scanning electron microscopy techniques were used to examine the powders. Image analysis software was used to determine quantitative data such as particle size and amount of melted and unmelted particles after PAS^{SM}. In addition, energy dispersive spectroscopy (EDS), Leco oxygen analysis, glow discharge mass spectroscopy, and inductively coupled plasma mass spectroscopy were used to determine compositional data about pre- PAS^{SM} (as-received) and PAS^{SM} powders.

Results and Discussion

Flow Analysis

Powder flow is critical because it affects process repeatability, which in turn determines a production technique's scrap rate. Highly flowable powders result in good repeatability and reduced scrap. Several characteristics affect powder flow including, but not limited to, morphology, density, particle size/distribution, and electrical properties. For metal powders, morphology has a major influence on flow, with spherical-shaped powder particles resulting in maximum flow characteristics.

Table 2 shows the results of Hall flow tests. All five refractory metal powders were tested in the as-received condition and after PAS^{SM} processing. Note that all powders in the as-received conditions resulted in no flow, i.e., failure of the test, which translates to inconsistent powder flow. In contrast, all PAS^{SM} powders passed the flow test, demonstrating excellent flow characteristics. PAS^{SM} powders demonstrated improved flow necessary for increased productivity and better repeatability during manufacturing.

Table 2: Hall flow test results for pre-PAS^{SM} (as-received) and PAS^{SM} powders.

Composition	Flowability (g/s)	
	As-received	PAS^{SM} processed
W	No flow (Failed)	100g/10s (Passed)
W-25Re	No flow (Failed)	100g/10s (Passed)
Mo	No flow (Failed)	50g/20s (Passed)
Mo-40Re Composite	No flow (Failed)	100g/15s (Passed)
Mo-40Re Coated	No flow (Failed)	50g/12.8s (Passed)

Tungsten Crystalline Powder

To baseline PAS^{SM}, initial experiments were conducted with tungsten crystalline powder. An SEM backscattered image of the as-received tungsten crystalline powder is shown in Fig. 1. This figure shows blocky, faceted powder morphology of the as-received tungsten powder. For comparison, Fig. 2 shows tungsten powder after PAS^{SM} processing. In contrast to the faceted particles of the as-received tungsten powder, the PAS^{SM} particles have a near perfect spherical shape, resulting in excellent flow characteristics. The beneficial spherical shape is formed as a result of surface tension forces due to particle melt as it is fed into the plasma. As the particle passes out of the plasma, the particle solidifies rapidly, which prevents distortion of the spherical shape as the powder is collected.

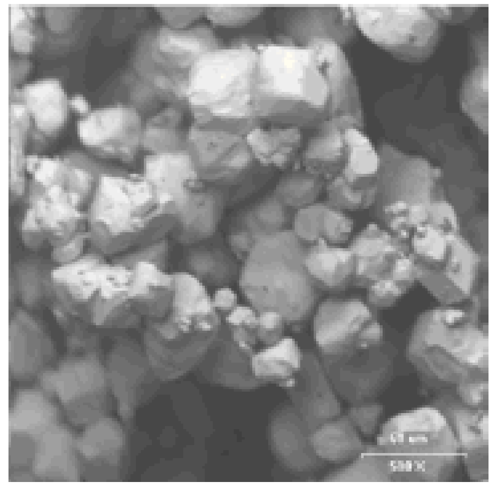

Figure 1: SEM backscattered image of as-received tungsten crystalline powder showing blocky, faceted powder particles (500x).

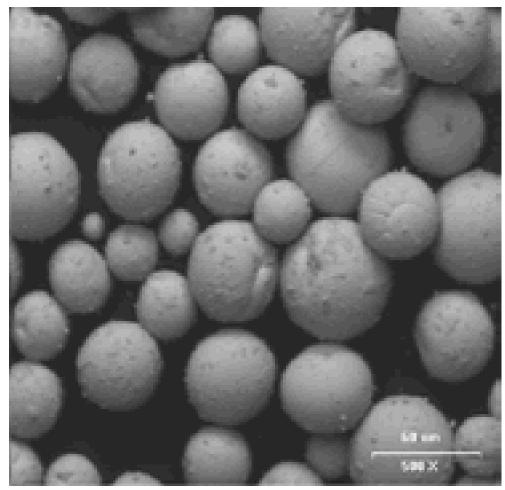

Figure 2: SEM backscattered image of tungsten crystalline powder after PAS^{SM} processing (500x). Highly spherical powder particles were produced.

W-Re Composite Powders

An SEM backscattered image of as-received W-25Re composite powder is shown in Fig. 3. The composite powder is comprised of large W particles (blocky/faceted morphology), smaller Re particles (flake-like morphology) and an organic binder. However, (as can be seen from Fig. 3) the as-received powder more closely resembles an elemental blend with few, if any, Re coated W particles. Figure 4 shows the same W-25Re powder after PAS^{SM} processing. Similar to the tungsten crystalline powder results, PAS^{SM} produces highly spherical W-Re particles with excellent flow characteristics. Because Re and W have similar densities ($\rho_{Re} = 21.0$ g/cm^3 and $\rho_W = 19.3$ g/cm^3), EDS analysis was unable to determine the composition of individual powder particles.

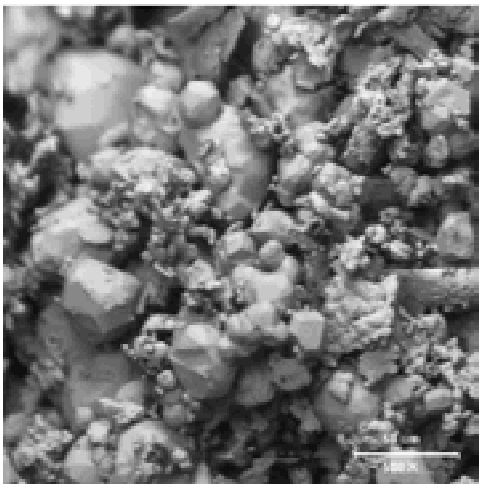

Figure 3: SEM backscattered image of W-25Re composite powder in the as-received condition (500x). The composite is comprised of blocky, faceted shaped W particles, flake-like Re particles and a 1-2% organic binder.

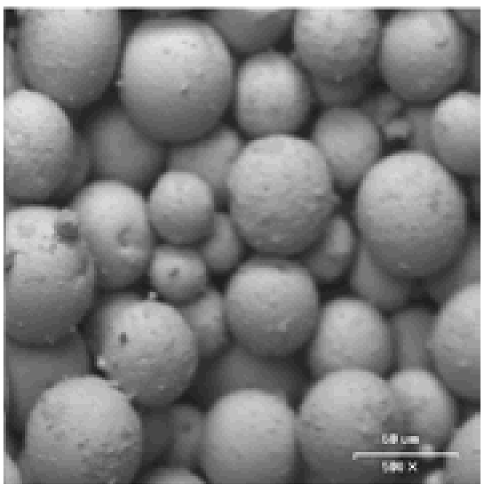

Figure 4: SEM backscattered image of W-25Re powder after PAS^{SM} processing (500x). PAS^{SM} produces highly spherical, W-25Re powder particles.

Spray Dried Molybdenum Powder
Spray-dried Mo powder was evaluated to determine the effect PAS^{SM} has on spray-dried powder. Figure 5 shows an SEM backscattered image of as-received spray-dried Mo powder. Note each powder particle is comprised of many smaller particles agglomerated as a result of the spray-drying process. Although the agglomerated particles are primarily spherical in shape, the as-received powder possessed poor flow characteristics.

Figure 6 is an SEM backscattered image of the PAS^{SM} spray-dried Mo powder. PAS^{SM} eliminated the agglomerated particles and replaced them with solid Mo particles. Because each spray-dried particle is comprised of many smaller powder particles (<10μm diameter), the amount of surface area is significantly more for agglomerated particles as compared to solid particles of the same size. With oxygen sensitive materials such as the refractory metals, more surface area results in greater oxygen contamination. Therefore, a spray dried Mo particle will have much higher oxygen content than a solid Mo particle of the same diameter. The Chemical Analysis section details lower oxygen content for PAS^{SM} Mo-40Re powders. Components made from PAS^{SM} powders will have lower oxygen contents, translating to better properties and improved performance.

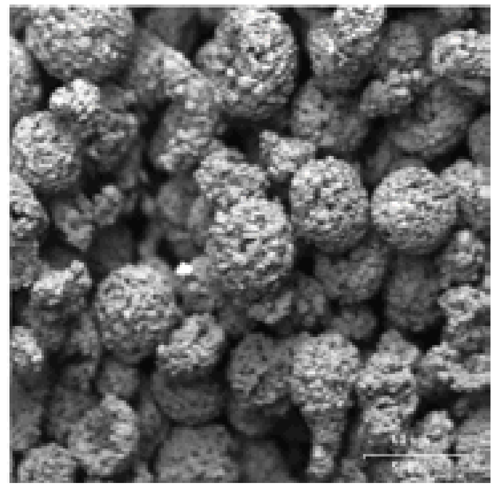

Figure 5: SEM backscattered image of spray-dried Mo powder in as-received condition (500x). Each spray-dried particle is comprised of smaller (<10μm particle diameter) agglomerated particles.

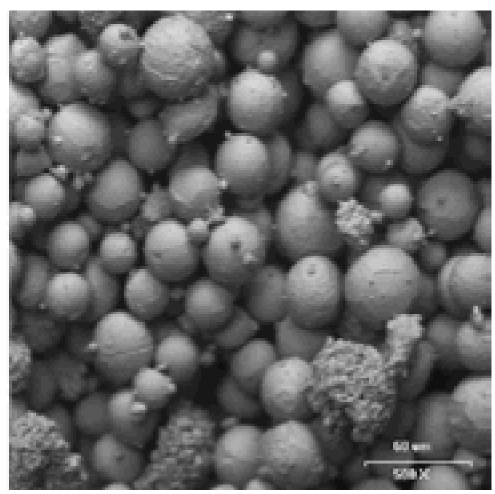

Figure 6: SEM backscattered image of PAS^{SM} spray-dried Mo powder after processing (500x). Note the agglomerated particles of as-received powder are converted to solid Mo particles, significantly reducing overall surface area and oxygen content.

Mo-40Re Composite Powder

Due to the large difference in densities of Mo and Re (ρ_{Mo} = 10.2g/cm^3 and ρ_{Re} = 21.0g/cm^3), compositional information was obtained from SEM backscattered images and EDS analysis for the Mo-40Re powder. Figure 7 is an SEM backscattered image of Mo-40Re composite powder in as-received condition. The lighter gray, flake-like particles are Re, while the darker gray, agglomerated particles are Mo. Figure 8 is an SEM backscattered image of a cross-section of as-received Mo-40Re powder. The cross-sectional image clearly shows the presence of porosity in agglomerated Mo particles and a non-uniform distribution of smaller, flake-like Re. The latter case has a significant effect on the ability to produce individual pre-alloyed particles with proper chemical composition.

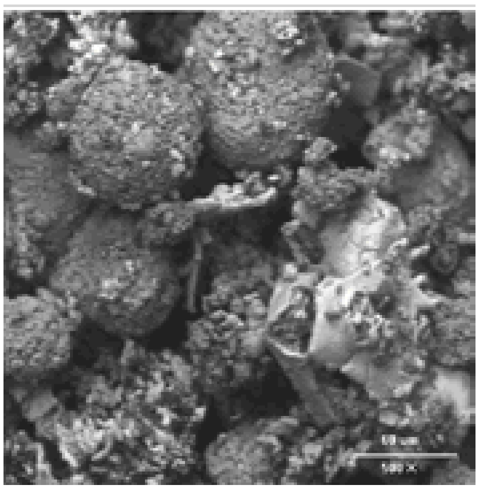

Figure 7: SEM backscattered image of as-received Mo-40Re composite powder (500x).

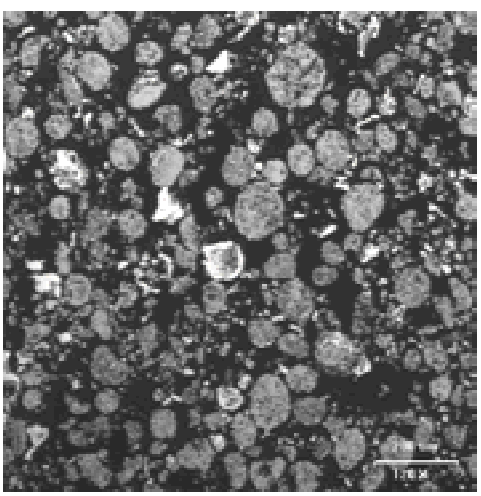

Figure 8: SEM backscattered cross-sectional image of as-received Mo-40Re composite powder showing non-uniform contact of Re flakes with spray dried Mo particles (120x).

An SEM backscattered image of cross-section PAS^{SM} Mo-40Re is shown in Fig. 9. Similar to previously discussed powders, PAS^{SM} produces highly spherical, dense Mo-40Re particles. Because of the density difference between Mo and Re, the backscattered image also reveals compositional information about each powder particle, i.e., light gray particles are Re-rich, dark gray particles are Mo-rich and medium gray particles have a composition between that of the light and dark particles. Figure 10 is a high magnification image of an individual particle. This figure demonstrates that each particle contains some amount of Re and Mo.

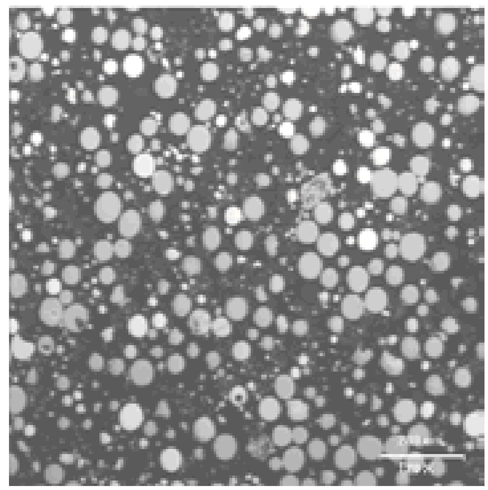

Figure 9: SEM backscattered image of cross-sectional view of PAS^{SM} Mo-40Re powder showing highly spherical, dense particles produced with the PAS^{SM} process (120x).

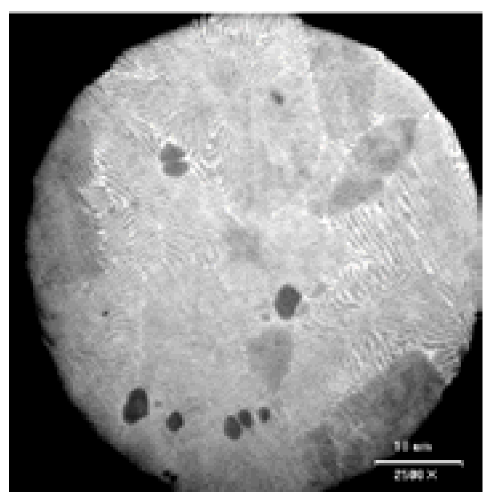

Figure 10: High magnification (2500x) SEM backscattered image of Mo-40Re powder after PAS^{SM} processing showing evidence that Re and Mo are present in each particle.

To estimate the amount of Re and Mo in individual particles, EDS analysis was performed on a dark gray, medium gray, and light gray particle. The spectra produced from this analysis are shown in Figs. 11-13. A comparison of the resulting peak heights is used as a qualitative estimate of each particle's chemical composition. The estimated chemical compositions for the dark gray, medium gray and light gray particles are Mo-19Re, Mo-45Re and Mo-78Re, respectively. A plausible explanation for these chemistries being skewed from the Mo-40Re bulk composition is non-uniform distribution of Re in the individual starting composite powder, i.e., variations within the nominal Mo-Re batch. Even without a uniform Re distribution, the analysis revealed significant amounts of Re alloyed with Mo in each PAS^{SM} particle.

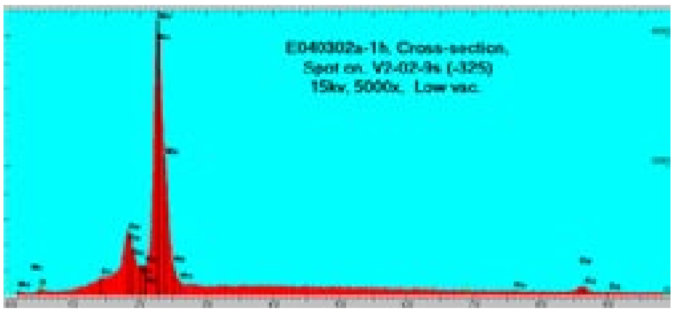

Figure 11: EDS spectrum of a dark gray Mo-Re particle after PAS^{SM} processing. Estimated particle composition: Mo-19Re.

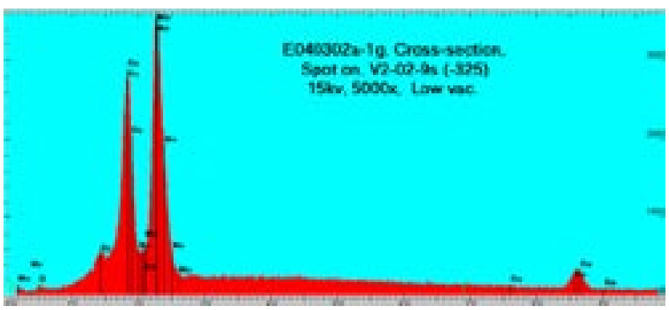

Figure 12: EDS spectrum of a medium gray Mo-Re particle after PAS^{SM} processing. Estimated composition: Mo-45Re.

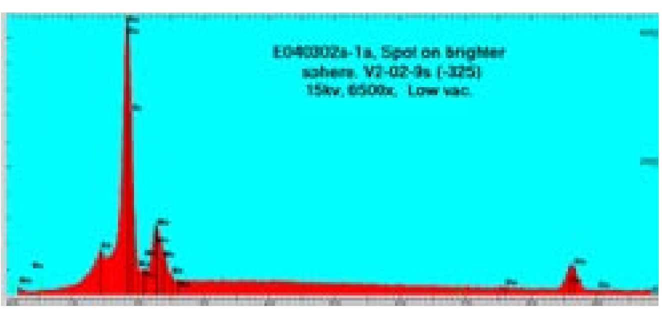

Figure 13: EDS spectrum of a light graph Mo-Re particle after PAS^{SM} processing. Estimated composition: Mo-78Re.

Mo-40Re Coated Powder

To produce individual powder particles with a similar composition as the bulk powder, coating of Mo particles with Re was evaluated. Figure 14 is an SEM backscattered image of Mo-40Re coated powder in the as-received condition. In contrast to as-received Mo-40Re composite powder, the as-received coated powder shows a more uniform distribution of rhenium among the powder particles before PAS^{SM}. The Re is not present as a separate phase, but as a coating on the spray-dried Mo particles. A cross-sectional view of an individual powder particle (Fig. 15) clearly shows a Re coating on a Mo powder particle. Re and Mo are in much closer contact in this powder than in any of the Re containing powders previously discussed.

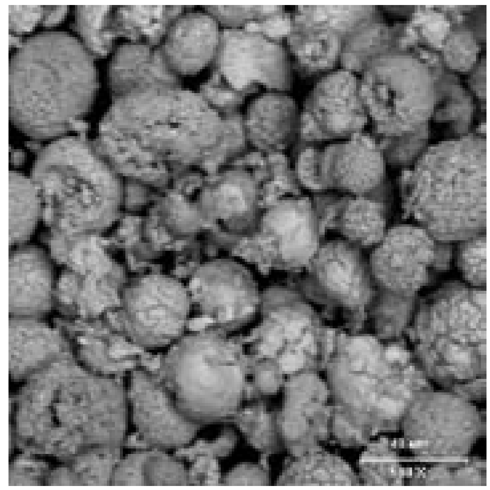

Figure 14: SEM backscattered image of as-received Mo-40Re coated powder (500x).

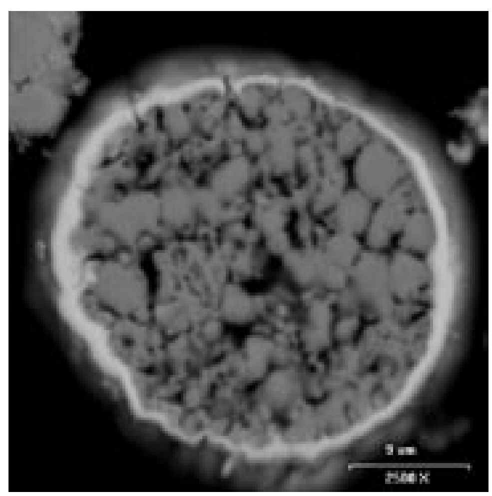

Figure 15: SEM backscattered cross-sectional image of as-received Mo-40Re coated powder particle at 2500x. The Re forms a shell around the porous Mo.

Figure 16 is an SEM backscattered image showing the Re coated Mo powder after PAS^{SM} processing. Similar to the previous samples, highly-spherical particles were produced. An SEM backscattered cross-sectional view of this powder is shown in Fig. 17. The lack of color differentiation among the particles indicates that each particle has a similar composition. This result is in contrast to that of PAS^{SM} processed Mo-40Re composite powder with individual particles rich in either Re or Mo (i.e., light and dark colored particles, respectively, in Fig. 9).

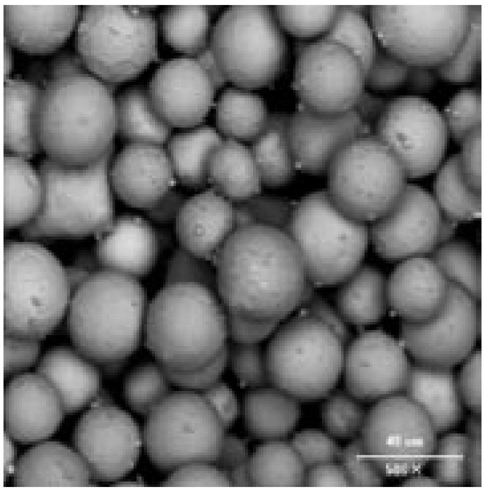

Figure 16: SEM backscattered image of PAS^{SM} Mo-40Re coated powder (500x). Note the spherical shape and uniform color of the powder particles.

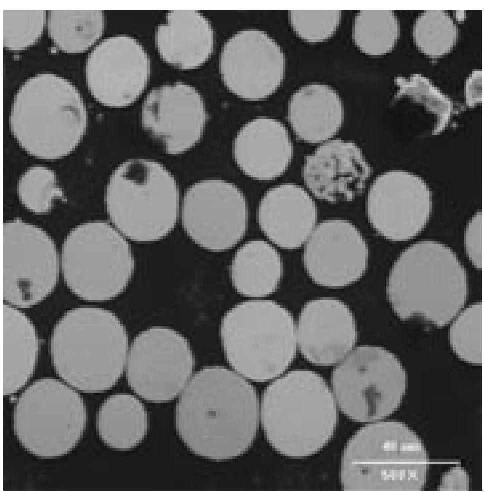

Figure 17: SEM backscattered cross-sectional view of PAS^{SM} Mo-40Re coated powder (500x). Note the spherical shape and uniform color of the particle cross-sections, indicating uniform composition (Compare to Fig. 9).

Using EDS analysis, the amount of Re in the individual particles was determined for PAS^{SM} processed Re coated Mo powder (Fig. 18). Based on the height of the Re peak, the percentage of Re was estimated to be 43-44% for the individual particles. Mass spectroscopy analysis of the bulk PAS^{SM} Mo-40Re coated powder showed the overall composition to be 40.0%Re and 59.8%Mo, plus trace elements. These results demonstrate the ability of PAS^{SM} processing to produce alloyed individual particles with a similar composition to the bulk powder composition.

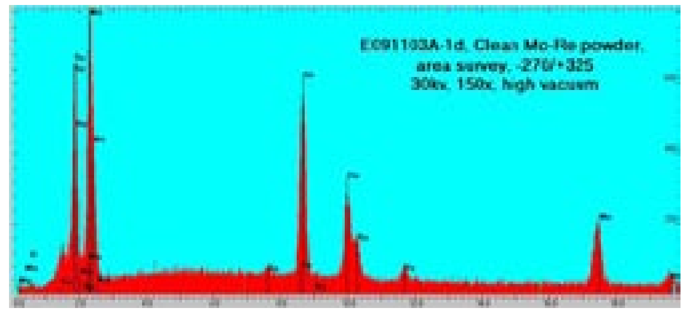

Figure 18: EDS analysis of 45-53 micron Mo-40Re coated powder after PAS^{SM}. This size fraction is representative of all size fractions, with estimated composition of 43-44% Re.

Chemical Analysis of PAS^{SM} Powders

Glow discharge mass spectroscopy and oxygen analysis showed no major pickup of impurities for Mo-40Re PAS^{SM} powders compared to as-received materials (see Table 3). A comparison of oxygen contents in the as-received composite/coated Mo-40Re compared to its PAS^{SM} counterpart showed significant decreases in oxygen. The reduction in oxygen content is due to use of a reducing plasma.

Table 3: Results of chemical analyses showing a reduction of impurities in PAS^{SM} processed Mo-40Re powders (ppm).

Mo-40Re	Ni	Cu	Cr	Al	Fe	O
As-received Composite*	300	100	100	<100	700	13000
PAS^{SM} Composite*	300	<100	200	<100	600	400
As-Received Coated *	50	12	70	100	490	8286
PAS^{SM} Coated *	24	4.1	19	35	265	2045

*Average of 4 measurements.

Ti-6Al-4V Powder

To verify the feasibility of PAS^{SM} processing for metal powders that are highly susceptible to oxidation, a titanium alloy (Ti-6Al-4V) was evaluated. The as-received Ti-6Al-4V powder was crushed, with many sharp, jagged edges and fragments (Fig. 19). In contrast, the PAS^{SM} Ti-6Al-4V powder contains mainly spherical particles (Fig. 20). The flow properties and chemical composition of the pre-PAS^{SM} and PAS^{SM} Ti-6Al-4V powders are currently being determined. However, when the micrographs are compared to those of W-25%Re and Mo-40%Re powders, an increase in flow, at the minimum, is anticipated. In addition, visual examination of the powder after PAS processing showed no sign of surface oxidation on the particles.

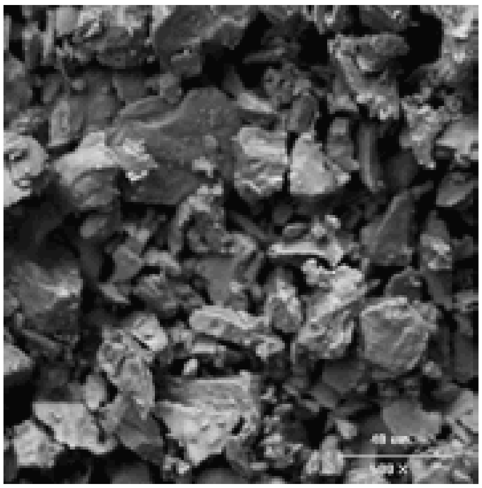

Figure 19: SEM backscattered image of Ti-6Al-4V alloy showing crushed, jagged edged powder particles at 500x.

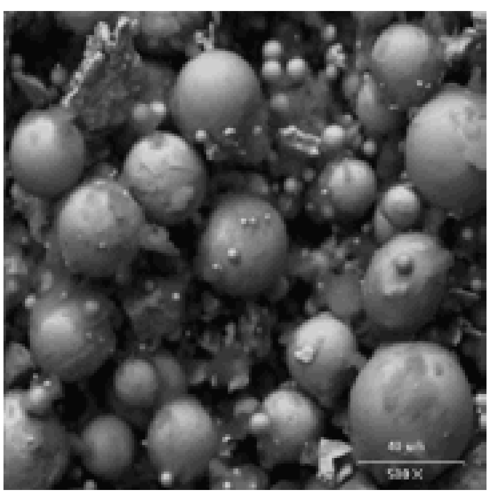

Figure 20: SEM backscattered image of PAS^{SM} Ti-6Al-4V alloy showing a majority of spherical powder particles at 500x.

Summary and Conclusions

Highly spherical refractory metal powders were produced possessing excellent flow characteristics using the PAS^{SM} process.

Pre-alloyed powders can be produced using the PAS^{SM} process.

Non-refractory metals, such as Ti-6Al-4V, can be spheroidized using the PAS^{SM} process.

Reduction in oxygen content of PAS^{SM} processed powder as compared to starting feedstock is possible.

No significant pickup of impurities was observed for PAS^{SM} processed powders.

Benefits of PAS^{SM} include; a reduction in oxygen content, production of highly spherical powders with enhanced flow characteristics, and the ability to produce pre-alloyed powders.

Acknowledgements

This work was supported through NASA's Small Business Innovative Research (SBIR) program under contract number NAS8-01157.

References

1. J.S. O'Dell, T.N. McKechnie, R.R. Holmes, *Development of Near Net Shape Refractory Metal Components Utilizing Vacuum Plasma Spray, Tungsten, Refractory Metals and Alloys 4, Metal Powder Industries Federation*, 159-166 (1998).
2. A. Agarwal, R. Hickman, T.N. McKechnie, J.S. O'Dell, *Advances in Near Net Shape Forming and Coating of Erosion Resistant Ultra High Temperature Materials*, *Tri-Service Sponsored Symposium on Advancements in Heatshield Technology*, Huntsville, AL May 10-11, 2000.
3. R. Hickman. T.N. McKechnie, J.S. O'Dell, *Material Properties of Net Shape, Vacuum Plasma Sprayed Rhenium and Tungsten, 39th AIAA/ASME/SAE/ASEE Joint Propulsion Conference,* Huntsville, AL, July 20-23, 2003.
4. T.A Leonhardt, U.S. Patent 6,551,377
5. J.S. O'Dell, *Robust, High Temperature Containment Cartridges for Micorgravity, NASA Final Report, Contract Number: NAS8-01157*, May 2002.